Seismic Site Amplification of the Cross of Opak River Fault at Yogyakarta, Indonesia, Under Ground Motions Generated by the Probabilistic Seismic Hazard Analysis

Widodo Pawirodikromo
Universitas Islam Indonesia
Mochamad Teguh
m.teguh@uii.ac.id
Islamic University of Indonesia: Universitas Islam Indonesia https://orcid.org/0000-0003-2709-3975
Lalu Makrup
Universitas Islam Indonesia
Mas Anggit
Universitas Islam Indonesia
Bambang Suryo
Universitas Islam Indonesia

Research Article

Keywords:

Posted Date: August 29th, 2025

DOI: https://doi.org/10.21203/rs.3.rs-7075085/v1

Seismic Site Response Across the Opak River Fault, Yogyakarta, Based on Probabilistic Seismic Hazard

Widodo Pawirodikromo[1], Mochamad Teguh[1], Lalu Makrup[1], Mas Anggit[1], Bambang Suryo[2]

[1]Department of Civil Engineering, Islamic University of Indonesia, Yogyakarta
[2]Alumni Master Program, Department of Civil Engineering

Abstract: This study assesses the extent of soil amplification and ground acceleration induced by an earthquake. Four locations were selected as study sites: Andi Jaya, Masjid Btl, Sabdodadi, and Imogiri boreholes along the Opak River fault. Since no earthquake records exist for these sites, ground acceleration was estimated using a single-site study approach based on the Probabilistic Seismic Hazard Analysis (PSHA) method. The Uniform Hazard Spectrum (UHS) at the bedrock level, derived from PSHA, was then adjusted to the risk-targeted earthquake level (UHS MCEr) by incorporating the directivity factor (Dr) and the risk-targeted factor (R). The matched accelerogram at the bedrock level was obtained by aligning the 1981 Corinth earthquake (Greece) with UHS MCEr. Site response analysis was conducted using the DEEPSOIL software, propagating the matched accelerograms vertically through the four borehole soil layers. The results indicate that the ground accelerations obtained were 0.347g, 0.344g, 0.341g, and 0.411g for the Andi Jaya, Masjid Btl, Sabdodadi, and Imogiri boreholes. The highest ground acceleration was recorded at Imogiri, as it is closest to the Opak River fault. The peak-to-peak ground acceleration amplifications were 1.66, 1.46, 1.30, and 1.49, while the peak-to-peak spectral amplifications were 2,206, 1,650, 1,702, and 1,616 for the respective boreholes.

1. Background

The primary objective of this study is to investigate bedrock acceleration, soil layer response, ground surface acceleration, and amplification at sites across the Opak River fault following the May 27, 2006, Yogyakarta earthquake, which resulted in significant human casualties. The Opak River fault in Yogyakarta Special Province (YSP), Indonesia, has not been extensively studied due to its relatively recent identification. The fault was first recognized following the Mw 6.1 Yogyakarta earthquake on May 27, 2006.

Historically, the Opak River fault was suspected following the Mw 7.7 Yogyakarta earthquake on May 28, 1867. This suspicion arose from the distribution of high Modified Mercalli Intensity (MMI) values observed near the present-day Opak fault [Nguyen et al., 2019; Sutiono et al., 2018]. However, the precise epicenter coordinates remain uncertain. The 1867 earthquake was not a shallow crustal event caused by Opak fault activity but a Benioff earthquake with a depth of 105 km. This condition is evident from its widespread impact, which affected all Central Java, most of East Java, and parts of West Java.

The Yogyakarta earthquake has been well-documented since the Mw 7.0 event on May 27, 2006, which caused severe damage with an intensity of MMI VIII [BMKG1, 2019]. The epicenter was located at 8.59°S, 109.80°E, with a depth of 60 km, approximately 109 km south of Yogyakarta. Another significant earthquake occurred on January 13, 1981 (Mw5.6), with an epicenter at 8.76°S, 110.43°E, and a depth of 51 km. However, this earthquake had a lesser impact on Yogyakarta due to its 108 km epicenter distance and maximum intensity of MMI VII [BMKG2, 2020]. In contrast, the Mw6.3 shallow crustal earthquake on May 27, 2006 [Tsuji et al., 2008], occurred much closer to Yogyakarta. While different sources report slightly varying epicenter locations [Elnashai et al., 2006], the USGS identified it at 7.96°S, 110.46°E. The epicenter was only about 26 km from Yogyakarta, with a shallow depth of 12 km, resulting in a maximum observed intensity of MMI IX [Widodo, 2018, 2020].

Historically, the 1867 earthquake in Yogyakarta caused an estimated 500 fatalities, including 12 Europeans [Nguyen et al., 2019]. The 1943 earthquake resulted in 243 deaths [BMKG1]. Meanwhile, the 2006 Yogyakarta earthquake led to 4,659 casualties, with 88.45% (4,121 deaths) occurring in the Bantul District. The disaster also caused the collapse of 88,249 houses across Yogyakarta Special Province, with 53% of the collapsed structures in Bantul. This high seismic vulnerability in Bantul is primarily due to shallow crustal earthquakes, as the district is directly adjacent to the Opak River fault (Fig. 1). Data analysis suggests a strong correlation between building collapse and human casualties during the 2006 Yogyakarta earthquake [Bappenas, Widodo, 2018]. The highest fatalities and structural failures occurred in Imogiri, Jetis, Bantul, Pundong, Bambanglipuro, and Sewon sub-districts along the Opak River fault. Therefore, investigating the seismic site response in this region is crucial.

As indicated in the study title, the site response analysis aims to determine (a) Ground acceleration at the bedrock level, (b) soil amplification, (c) ground acceleration at the surface level, and (d) the dynamic response of soil layers at the site. Previous research on ground motion in Yogyakarta City utilized deterministic, microtremor, and site response analysis (NERA) methods [Fathani & Wilopo, 2017]. The results showed maximum ground acceleration values of 0.14–0.21 g (deterministic), 0.05–0.30 g (microtremor), and 0.19–0.38 g (NERA). However, a limitation of this study was that the bedrock ground acceleration (0.25g) for site response analysis (NERA) was determined based solely on amplification maps and soil conditions in Yogyakarta without considering variations across different locations. Additionally, this research did not analyze soil layer amplification or dynamic response.

Further research on ground acceleration in YSP, including Bantul, was conducted by Widodo (2018, 2020). The study found that the maximum ground acceleration near the earthquake source ranged between 0.40 and 0.50 g. Field studies using microtremor methods have identified areas across and west of the Opak fault with deep sedimentation zones [Daryono, 2011; Widodo, 2020], contributing to seismic site effects. However, this research also had limitations, as the ground acceleration values were estimated based on observed MMI values rather than direct measurements of soil amplification and dynamic response.

Given these research gaps, improving the quality of seismic studies is essential. Since direct earthquake records are unavailable for the study area, bedrock acceleration is determined by matching the risk-targeted Uniform Hazard Spectrum (UHS MCEr) using the Probabilistic Seismic Hazard Analysis (PSHA) method. Unlike previous studies, which used deterministic approaches for the entire research area, this study determines UHS through a single-site analysis, ensuring that the UHS MCEr is specific to each investigated point. The site response analysis propagates one-dimensional shear wave motion to the ground surface, allowing for the accurate determination of site amplification and ground acceleration at each location.

2. The Tectonics and Geology of the YSP

Tectonics is generally defined as the movement of the Earth's lithosphere, which consists of its rigid outermost layer or shell. Tectonically, the Yogyakarta Special Province (YSP) is situated on the island of Java, which is part of the Eurasian Plate (Fig. 1). This plate moves southward and collides with the Australian plate at the plate boundary, which moves in the opposite direction. The subduction zone at this plate boundary is approximately 325 km south of Yogyakarta City [Widodo, 2019] and has triggered megathrust, Benioff, and shallow crustal earthquakes, as mentioned earlier.

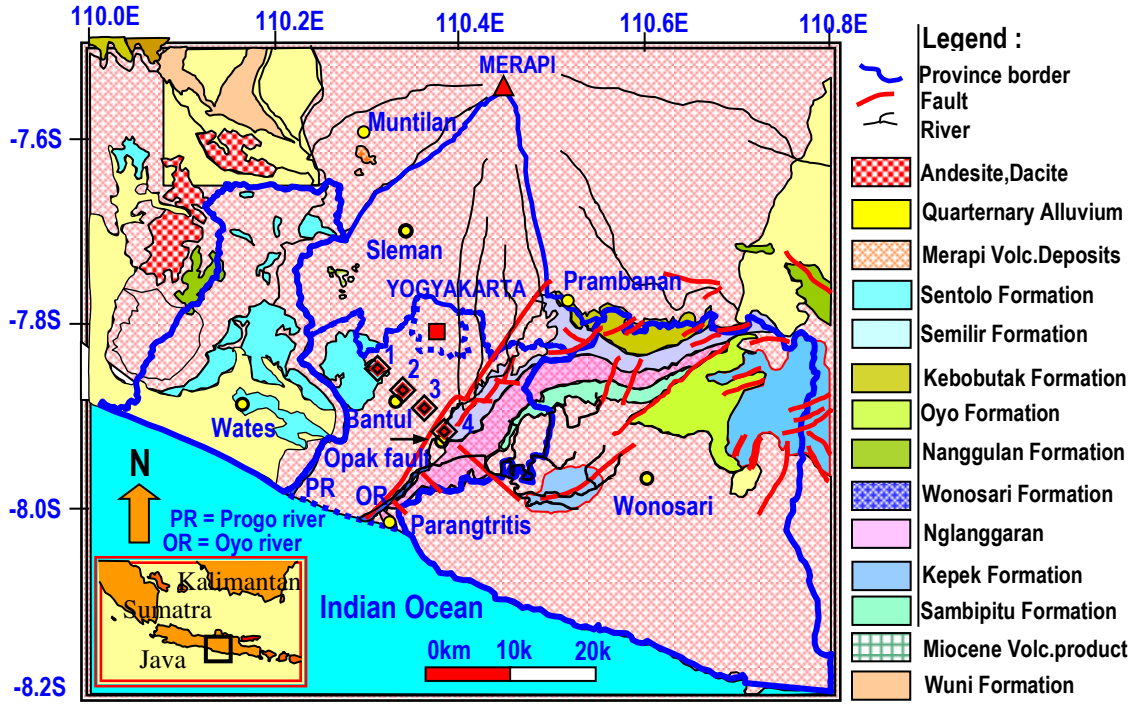

Fig.1. Local geology map of Yogyakarta Special Province, YSP [Modified Handayani, 2019]

As shown in Fig. 1, the Yogyakarta Special Province (YSP) comprises four districts and one municipality. Sleman Regency is in the north, while the southern regions of Gunungkidul (Wonosari), Bantul, and Kulonprogo (Wates) districts form a plain with gentle slopes that extend to the Indian Ocean coast. At the northern end of YSP stands Mount Merapi, an active volcano with an elevation of 2,930 meters (9,613 feet) above sea level.

Regarding regional geology, rocks, and soils in YSP began during the Tertiary and Quaternary periods [Kyaw et al., 2014]. As illustrated in Fig. 1, the western parts of Kulonprogo and Gunungkidul districts are characterized by mountain ranges with rock formations dating back to the Tertiary period. These formations include the Semilir and Nglanggaran Formations**,** Sambipitu Formation (sandstone)**,** and Sentolo and Nanggulan Formations (limestone) [Handayani, 2019].

In the northern region, particularly Sleman Regency, which is closest to the slopes of Mount Merapi, the soil profile consists primarily of coarse sand and gravel deposited over time through successive volcanic eruptions. In contrast, the southeastern parts of Kulonprogo and most of Bantul District are valley areas where soils formed during the Quaternary period. These deposits mainly consist of fine sand, clay, and silt, resulting from the weathering of Tertiary sedimentary rocks [Nurwihastuti et al., 2014]. The soils in these areas are relatively young and thick, making them highly susceptible to seismic vulnerability **[**Daryono, 2011].

3. Probabilistic Seismic Hazards Analysis (PSHA)

3.1 Uniform Hazard Spectrum (UHS)

The history of the Development of PSHA cannot be separated from the concept developed by Cornell and Esteva in the 1970s [McGuire, 2008]. At the time, the relationship between earthquake return period T and ground motion parameters was initially introduced by Cornel (1968) in the context of risk analysis. Meanwhile, Esteva developed a linkage between the ground motion parameters (PGA, PGV, and PGD) and magnitude and distance, which enabled the creation of a seismic zone map for the first time. The concept of the 2-scientist collaboration eventually led to the PSHA, which was then methodically adopted by many countries.

Finally, step-by-step guidance on understanding PSHA can be found in various publications, including Baker's (2008). In PSHA, a hazard parameter X is generally used (for example, ground acceleration). The probability of an earthquake occurrence was calculated for the value of X > x, or mathematically written as P (X > x). In the probability determination of exceeding a specified ground motion amplitude x, a prescribed hazard needs to be integrated for all possible earthquake magnitude M, distance R, and earthquake source through the total probability theorem through the formula [Kijko,2011]:

$$\lambda_X(x) = \sum_{i=1}^{n} \nu_i (M > m_{\min}) \int_M \int_R P_i (X > x \mid m, r)\ f_{M,i}\ f_{R,i}\ dr\, dm \tag{1}$$

where v (M > mmin) is the annual earthquake rate of occurrence greater than minimum magnitude mmin, P (IM >x|m,r) is the probability of intensity measure X greater than x caused by variables earthquake magnitude m and distance r, fM and fR respectively are cumulative probability function of m and r.

Eq. (1) yields a graph of the relationship between the annual rate of exceedance, lX(x), and ground acceleration. If a specific value, lX(x), is applied to all spectrum periods T, then a Uniform Hazard Spectrum (UHS) graph will be obtained. The UHS obtained is based on a single-site analysis process at a point under consideration, where v (M > m_{min}) is the annual earthquake rate of occurrence greater than minimum magnitude m_{min}, P (IM >x|m,r) is the probability of intensity measure X greater than x caused by variables earthquake magnitude m and distance r, f_M and f_R respectively are cumulative probability function of m and r.

Eq. (1) produces a graph of the relationship between the annual rate of exceedance, X (x), and ground acceleration. If a specific value, X (x), is then taken and applied to all spectrum periods T as used, a Uniform Hazard Spectrum (UHS) graph will be obtained. The UHS obtained is based on a single-site analysis of the int under consideration.

3.2 Risk-Targeted Spectra Demand and Matched Ground Motions

The Ground Motion Prediction Equation (GMPE) used in the Probabilistic Seismic Hazard Analysis (PSHA) is the spectral demand obtained by the root of the product of two perpendicular acceleration records [Bradley, Baker, 2014]. This approach, however, does not consider the maximum spectral demand [Huang et al., 2008]. According to

their study, spectral response ratios for all orientations were presented, including the maximum value relative to the standard due to the directivity effects. In short, directivity effects need to be considered in spectral demand.

The UHS determined from PSHA is only the average or geometric mean spectral demand at the application level. The value of maximum spectral demand must be considered to accommodate the possibility of directivity effects, ensuring that the obtained UHS reaches the Maximum Credible Earthquake (MCE) level. The geometric mean and maximum spectral demand are then connected by a value called the directivity factor, which is the function of the period T [Sengara, Komerdevi, 2019].

According to the Indonesian Seismic Loading Code, the directivity factor for T = 0 s can be taken as Df = 1. For the period T = 0.2 s, the value of Df is 1.1, and for the period T = 1.0 s, the value of the directivity factor is 1.3. The Df value can be calculated linearly from T = 0 s to T = 0.2 s and from T = 0.2 s to T = 1.0 s. The directivity factor remains constant for T > 1.0 s, Df = 1.3 [Sengara and Komerdevi, 2019]. Apart from the value of the directivity factor, it is still necessary to know that at the MCE level, it cannot guarantee uniform building collapse for 50 years [Luco, 2011]. Therefore, one additional factor must be considered: the risk-targeted coefficient (Rf), so the ground motions reach the Risk-Targeted Maximum Credible earthquake (MCEr). Based on the Indonesian Seismic Code, the risk-targeted coefficient has been presented as a map, specifically a CRS map for a short period (T = 0.2 s) and a CR1 map for an extended period (T = 1.0 s).

Since there are no earthquake records, one earthquake record was selected from the USGS Catalog. The earthquake response spectrum is then matched with the targeted spectrum demand UHS MCEr, and a matched accelerogram is defined. The earthquake record was selected so that the earthquake-significant duration of D595 still fell within the range of values proposed by Kempton and Stewart [2009] and as presented by Widodo [2019]. The record of the Corinth North-South Component (NSC) earthquake that occurred in Greece on February 24, 1981, has been chosen because it has a significant duration of D595 = 20.27 s, still falling within the range of D595 = 13.04 s-24.63 s, as conveyed by Widodo (2019).

4. Boreholes and Site Response Analysis

The study area in this research has been identified as a deep sedimentary soil region, as stated by Daryono [2011] and Widodo [2020], particularly in the area that crosses the Opak River fault and extends through Bantul Regency. This region experienced a relatively high percentage of human casualties and housing collapses during the May 27, 2006, earthquake. This study requires data on soil layers, soil properties, groundwater levels, shear wave velocity, and bedrock depth. For this purpose, four boreholes were drilled across the Opak River fault, specifically at Andi Jaya (1), Masjid Btl (2), Sabdodadi (3), and Imogiri (4), as shown in Fig. 2.

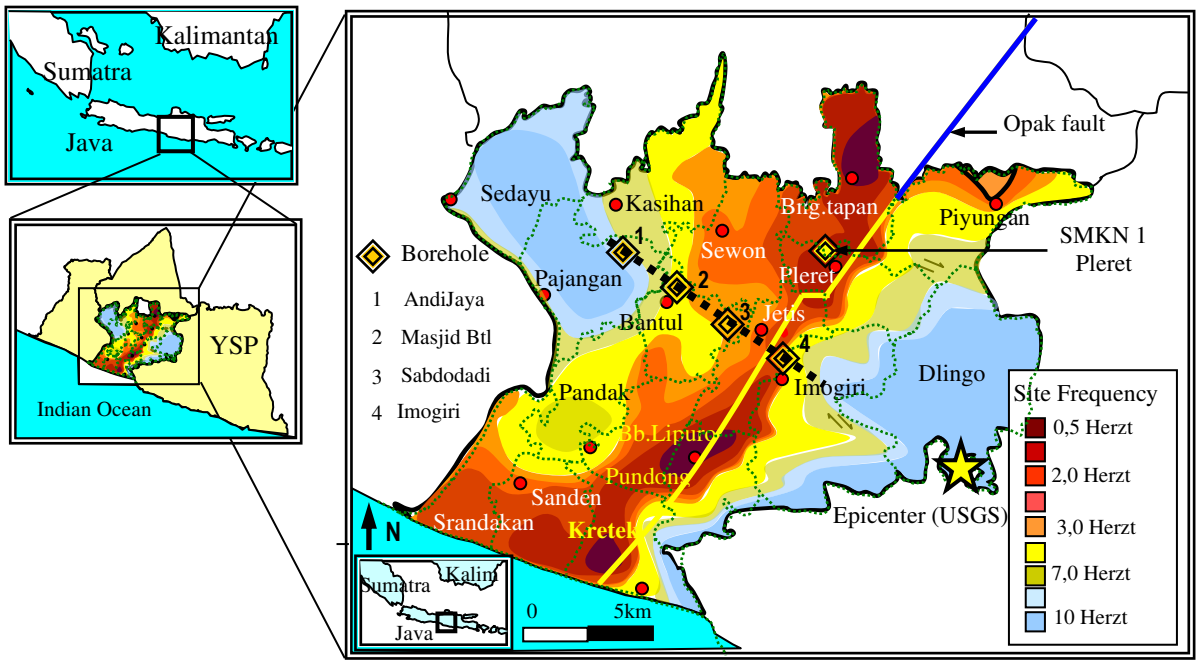

Fig.2. Borehole locations: (1) Andi Jaya, (2) Masjid Btl, (3) Sabdodadi and (4) Imogiri

The dynamic analysis of soil layers was conducted using DEEPSOIL software (Hashash et al., 2016). The study employed a 1-D model, considering time-domain nonlinear soil response while neglecting pore water pressure generation. In DEEPSOIL, the soil layer is modeled as a multi-degree-of-freedom lumped parameter system or a finite element system, where a mass, a nonlinear spring, and viscous damping represent each successive 0.5 m layer. The Masing rules soil constitutive model was applied to simulate the nonlinear hyperbolic behavior of soil [Hashash et al., 2010], generating hysteretic loops. Regarding model dimensioning, a comparison of surface spectral acceleration based on the Finite Difference Method (FDM) and Finite Element Method (FEM) in 1-D, 2-D, and 3-D models was conducted by Lopez et al. [2015]. The results indicate that spectral acceleration in 1-D is only slightly higher than in 2-D and 3-D models.

The number and thickness of soil layers, shear wave velocity (Vs), and all required soil properties for DEEPSOIL were determined from borehole data collected in the field. Since shear wave velocity (Vs) values for each layer were not directly obtained from field measurements, the empirical formula proposed by Hasancebi and Ulusay [2007], as presented by Akin et al. [2011], was used. In DEEPSOIL, soil mass is modeled as a lumped-mass multi-degree-of-freedom system. A horizontally layered soil deposit is subjected to vertically propagating horizontal shear waves at the base. The thickness of each soil layer has a significant influence on the site response [Anbazhagan, 2013]. This study used the actual layer thickness observed in the field.

5. Method of Investigation

5.1 Collection and Processing of Earthquake Data

The earthquake data used in this study were selected from the USGS Catalog, covering the period from 1963 to 2016 within a 500 km radius of Yogyakarta (Fig. 3). The data were processed by separating mainshocks from aftershocks and converting all magnitudes into a uniform unit.

5.2 Earthquake Source Identification and Software

As previously mentioned, the Australian Plate subducts beneath the Eurasian Plate approximately 325 km south of Java Island. The movement of the Australian Plate is almost perpendicular to the orientation of Java. As a result, Java does not have a massive series of earthquake faults, such as the Great Sumatra Fault on the Island of Sumatra. Based on past earthquake events and their impacts, the shallow crustal earthquake source is more dominant in this region. The Uniform Hazard Spectrum (UHS) generated by megathrust earthquakes is significantly lower than that produced by shallow crustal earthquakes [Widodo, 2019]. Therefore, this study focuses only on the shallow crustal earthquake source.

For example, one of the faults considered is the Cimandiri strike-slip fault, located in Cimandiri Bay, West Java (Fig. 3) [Nguyen et al., 2015]. The Cimandiri Fault, with a strike of N70°-80°, extends from Pelabuhan Ratu Bay through Sukabumi, Cianjur, and Bandung. It is approximately 100 km long and has a slip rate of 0.5–1.7 mm/year [Febriani, 2015], with a higher estimate of 4 mm/year [Irsyam et al., 2017]. Another relevant fault is the Bumiayu Fault in western Central Java, which extends the Baribis Fault. According to Sunardi [2016], the Bumiayu Fault is a right-lateral strike-slip fault with a dip angle of 90° and a slip rate of 2.0 mm/year. It was responsible for the 1995 earthquake in the region.

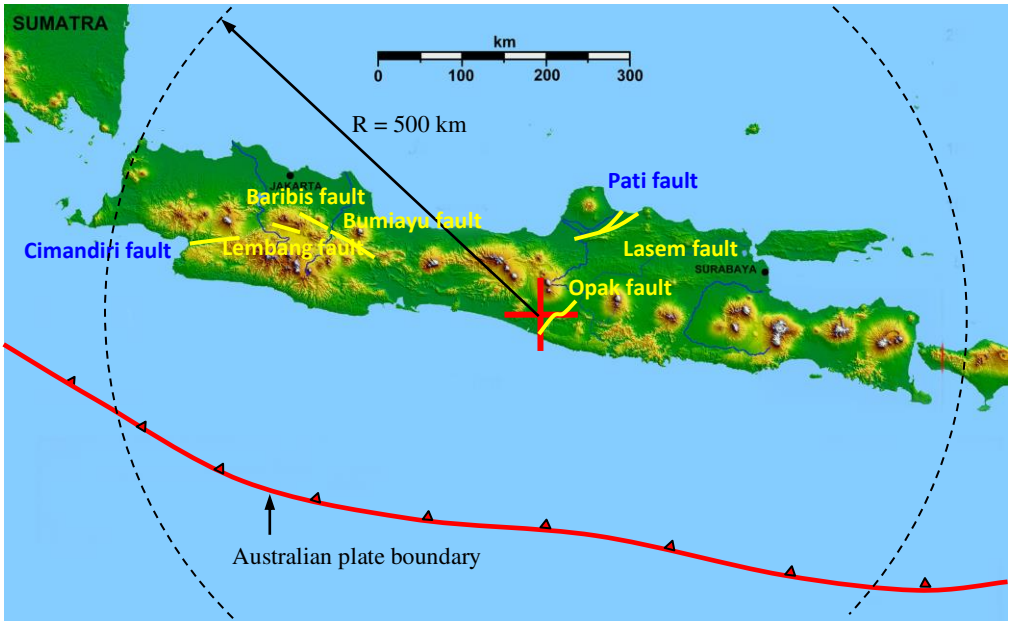

Fig.3. Shallow crustal source mechanism of the YSP.

Table 1. The data and parameter fault in Yogyakarta and Central Java [Sunardi, 2016]

No	Fault	Location	Slip-rate	Source mechanism	Fault length	M_{max}
1	Opak-Yogya	Yogyakarta	2.4 mm/year	Right strike-slip	31.6 km	6.8
2	Lasem	Central Java	0.5 mm/year	Strike-slip	114.9 km	6.6
3	Pati	Central Java	0.5 mm/year	Strike-slip	51.4 km	6.8
4	Bumiayu	Central Java	0.5 mm/year	Right strike-slip	44 km	6.0
5	Cimandiri	West Java	2.0 mm/year	Strike-slip	98 km	7.2
6	Baribis	West java	0.2 mm/year	Strike-slip	64 km	6,8
7	Lembang	West Java	2.0 mm/year	Strike-slip	30 km	6.6

In Central Java, the Lasem fault is an active fault that extends from the eastern part of the city of Semarang to the east, through the northern mountains of Purwodadi, and continues up to Lasem [Partono et al., 2017]. Meanwhile, the Pati fault is a branch of the Lasem fault, extending eastward from southern Kudus and Pati town to near Rembang. The data and parameters of the Lasem and Pati faults are presented in Table 1. Furthermore, for the implementation of the PSHA, a Computer Program Called SHModel [Makrup, 2009] was used. Performance verification of the software has been carried out, confirming that its output value aligns with the USGS Seismic Hazard Program output used by Pettersen et al. [2004] and EQRisk [2005], as used by Irsyam et al. [2008].

6. Results and Discussions

6.1 Soil Layers

The results of the field soil investigations, as determined by the Borehole Standard Penetration Test (N-SPT), are presented in Fig. 4. Following the completion of soil exploration, interpreting the results is necessary. The figure shows that the soil layers are generally regular and straightforward, except for borehole No. 1 in Andi Jaya. The soil type in the four boreholes is silty loam at the soil surface, although its thickness varies. The layers below, respectively, are fine sands, medium sandy loam, and silty clay, except for Andi Jaya's borehole. Almost uniformly, the next layer is sandstone, followed by limestone. This picture shows that the thickest sediment soil above the sandstone and limestone is in the Masjid Btl borehole, followed by the Sabdodadi and Imogiri boreholes, and the shallowest one, Andy Jaya. Besides soil properties and groundwater level depth, the thickness of the sediment soil will also affect the site response value.

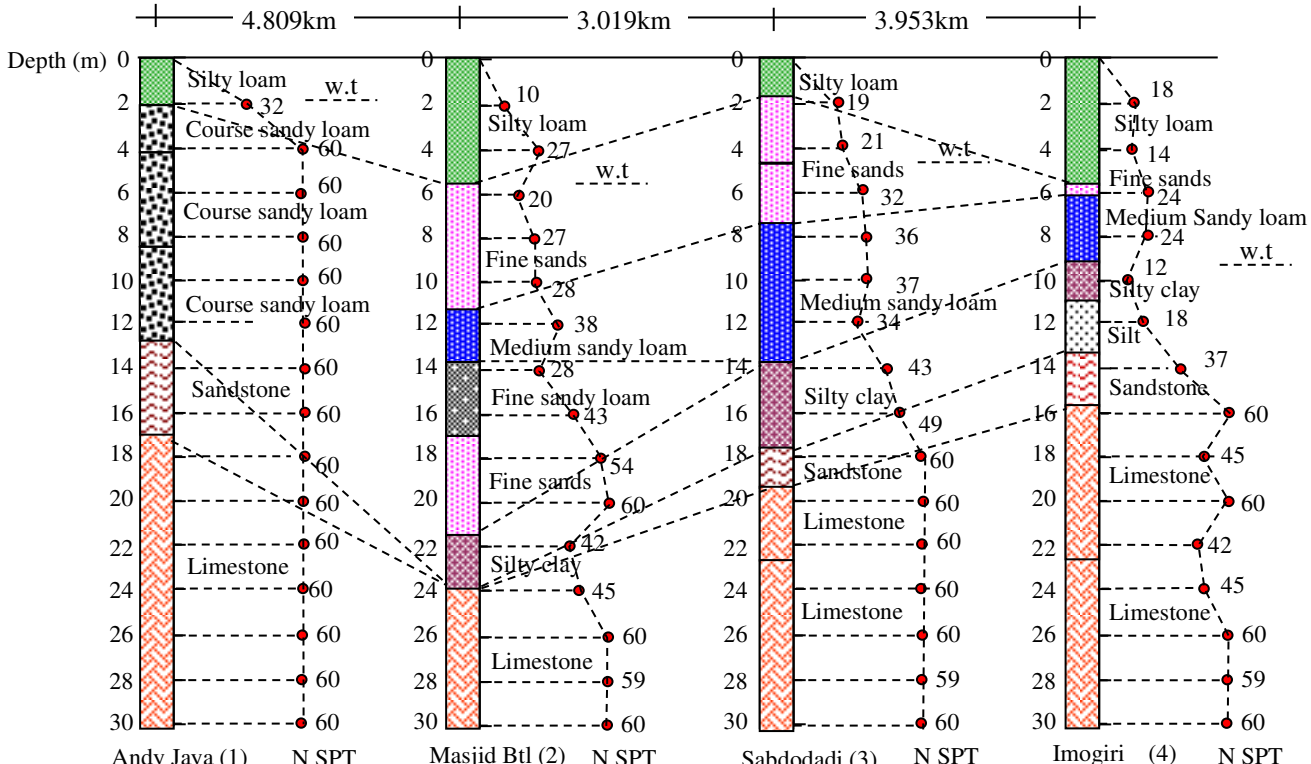

Fig.4. Soil profile at Andi Jaya, Masjid Btl, Sabdodadi, and Imogiri boreholes

Furthermore, the average values of N-SPT, shear wave velocity (Vs), and site period (T) must be calculated to determine the site classification. The results are presented in Table 2. According to BSN [2019] and Ji et al. [2017], the soil at the Andi Jaya borehole falls into the hard-soil (SC) category, whereas the soils at the Masjid Btl, Sabdodadi, and Imogiri boreholes are classified as medium soil (SD). This difference in site classification is due to geological variations, as shown in Fig. 1. The Andi Jaya borehole is located within the Sentolo Tertiary rock formation, whereas the other three locations, namely Masjid Btl, Sabdodadi, and Imogiri, are situated within Quaternary young volcanic deposits. The sedimentary soil at the Imogiri borehole is relatively soft and flexible, as indicated by the lowest average N-SPT and shear wave velocity (Vs) values. Conversely, it has the most significant site period (T). The Masjid Btl borehole contains the deepest sediment, with dynamic soil characteristics (N-SPT, Vs, and T) like those in Imogiri. Overall, the soil at all four boreholes is predominantly composed of sand layers derived from young volcanic deposits of Merapi. A surface layer of silty loam, formed from rock weathering deposits, is present.

Table 2. Average of N-SPT, Vs, and site period T

Description	Location			
	Andi Jaya (1)	Masjid Btl (2)	Sabdodadi (3)	Imogiri (4)
N(avrg)	56.93	31.13	39.89	29.12
Vs(avrg) m/s	314.443	268.31	286.10	265.45
T (s)	0.381	0.447	0.419	0.452
Category	Hard soil	Medium soil	Medium soil	Medium soil

6.2 The Targeted UHS Spectrum Demand

This study's Probabilistic Seismic Hazard Analysis (PSHA) output is the Uniform Hazard Spectrum (UHS) at the geometric mean level. As previously stated, this geometric mean spectral demand must be adjusted to the Maximum Credible Earthquake (MCE) level by incorporating the directivity factor (Df). Furthermore, the risk-targeted factor (Rf) is applied to transition from the MCE level to the risk-targeted spectral demand at the MCEr level to account for risk considerations.

The risk-targeted spectral demand at the MCEr level for the borehole locations, namely Andi Jaya (1), Masjid Btl (2), Sabdodadi (3), and Imogiri (4), is presented in Fig. 5, indicating that the distance from the Opak River fault influences the maximum MCEr spectral demand. As illustrated in Fig. 2, the Imogiri borehole is the closest to the fault, followed sequentially by Sabdodadi, Masjid Btl, and Andi Jaya, the farthest. Consequently, the maximum values of the MCEr spectral demand are as follows: Imogiri, 0.915; Sabdodadi, 0.780; Masjid Btl, 0.671; and Andi Jaya, 0.596. This trend confirms that locations closer to the Opak River fault experience higher seismic demand.

Similarly, the maximum Peak Ground Acceleration (PGA) follows a regular pattern corresponding to the distance from the epicenter of the fault. The closer the site is to the Opak River fault, the higher the matched or synthetic accelerogram PGA, and vice versa. The maximum PGA values obtained are Imogiri, 0.275 g; Sabdodadi, 0.262 g; Masjid Btl, 0.236 g; and Andi Jaya, 0.209 g. These matched or synthetic accelerograms will serve as input ground motions for site response analysis, where they will be used to simulate the vertically propagating horizontal shear wave within the layered soil deposits.

6.3 Nonlinear PGA and PGA Amplification

The soil amplification factor can be determined using earthquake records or site response analysis. This study's key research questions and primary outputs are Peak Ground Acceleration (PGA) and PGA amplification. The bedrock and ground surface accelerations for the four boreholes are presented in Fig. 6. The 1-D site response analysis results are relatively close to those obtained from 2-D and 3-D models, which aligns with the expected outcomes of this study. Among the four boreholes analyzed, the highest PGA at the soil surface is observed at Imogiri (0.411 g), followed by Sabdodadi (0.341 g). The PGA increases slightly at Masjid Btl (0.344 g) and Andi

Jaya (0.347 g). The Imogiri borehole records the highest PGA because of its proximity to the Opak River fault and the highest risk-targeted spectrum demand and PGA-matched acceleration values.

Fig. 6 also presents the PGA amplification at the four borehole locations. The most significant amplification occurs at Andi Jaya (1.66), where the PGA at bedrock is 0.209 g, and the PGA at the ground surface is 0.347 g. This amplification can be attributed to three factors: (1) a natural increase in earthquake frequency at the surface due to a change in the A/V ratio, which rises from 1.198 (medium frequency) at the bedrock level to 1.445 (high frequency), (2) the structure's response approaching resonance, as the soil at the Andi Jaya borehole is relatively complex, and (3) minimal shear strain in the soil layer, leading to negligible energy absorption. A lower energy absorption results in a more enormous response. The PGA amplification factors for the other boreholes are 1.49 (Imogiri), 1.46 (Masjid Btl), and 1.30 (Sabdodadi). Compared to the findings of Kaiser and Massey [2014], these PGA amplification values fall within the low-to-medium range and do not yet reach the high amplification category.

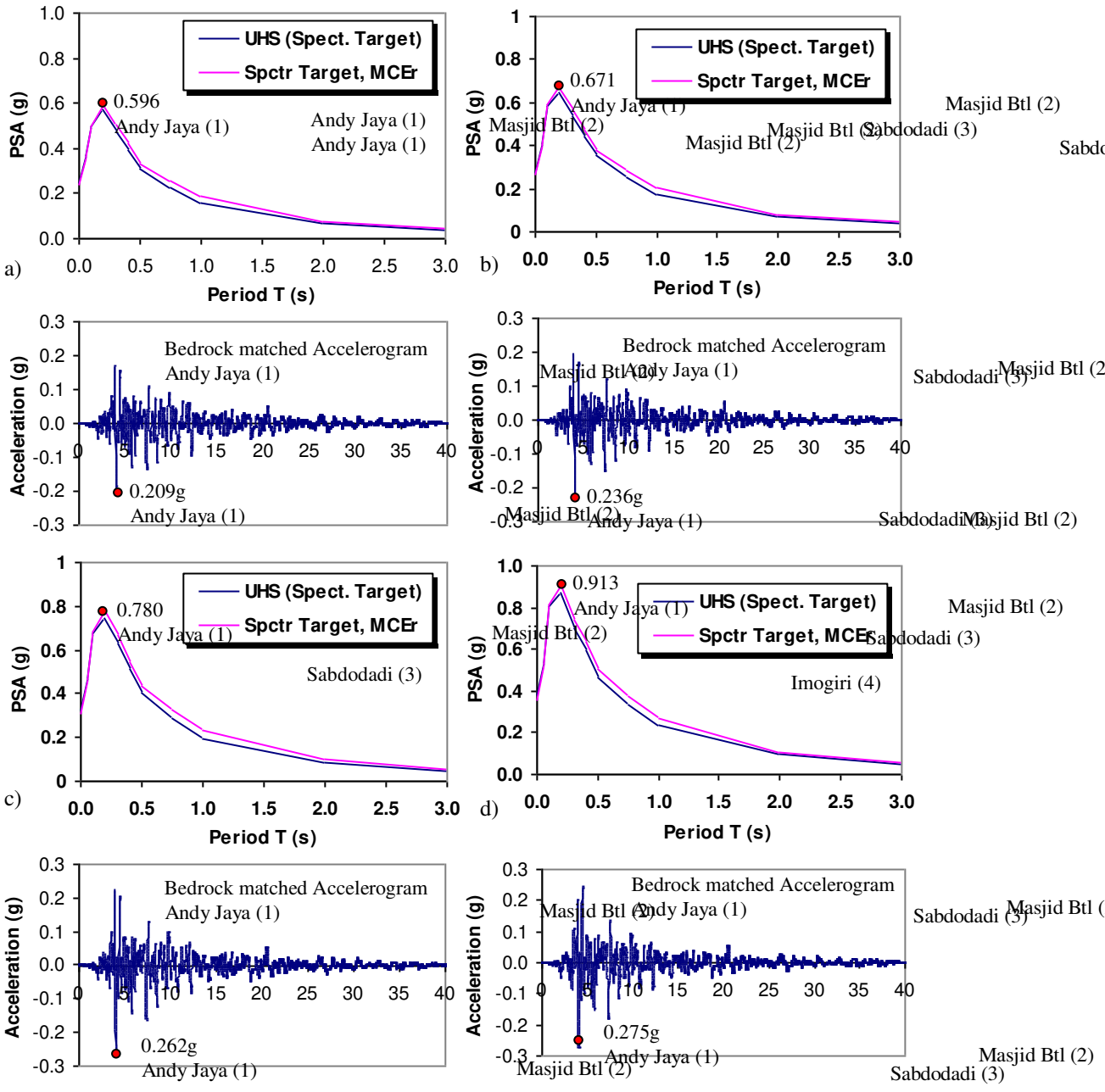

Fig. 5. Targeted UHS Spectrum demand and bedrock-matched or synthetic accelerogram.

6.4 Ground Acceleration and Ground Strain Profiles

Fig. 6 presents the ground acceleration at each soil layer of the four borehole locations. Consistent with previous results, the ground-level acceleration values were 0.347 g, 0.344 g, 0.341 g, and 0.411 g for Andi Jaya (1), Masjid Btl (2), Sabdodadi (3), and Imogiri (4), respectively. The highest ground acceleration was observed at borehole-4 (Imogiri) because it is closest to the Opak River fault's earthquake source.

As shown in Fig. 6, there is a clear tendency for acceleration amplification, with a noticeable increase in ground acceleration in the upper soil layers. The vertically propagating horizontal shear wave causes a decrease in the natural frequency of ground acceleration as it moves upward through the soil layers. This effect can be identified in the reduction in the A/V ratio (acceleration-to-velocity ratio) as the wave propagates toward the ground surface. For instance, in the Imogiri borehole, the A/V ratio decreases from 1.138 at the bedrock level to 1.124 at the ground surface. A similar trend was observed at the Sabdodadi borehole. However, the results for Andi Jaya and Masjid Btl boreholes showed the opposite trend, making these findings particularly interesting. At the Andi Jaya borehole, the A/V ratio increases from 1.198 (medium frequency) at the bedrock level to 1.445 (high frequency) at the ground surface. This phenomenon occurs because Andi Jaya has only a thin sediment layer, resulting in high acceleration, as reported by Seed and Idriss [1969].

Furthermore, the soil shear strain profile in Fig. 7 exhibits behavior different from ground acceleration. Since shear strain is calculated as the ratio of relative displacement to layer thickness, it is analyzed at the soil mass level for each layer. In the lumped mass model, horizontal mass displacement follows a shear building displacement pattern, where the relative displacement is most prominent at the bottom layer and least prominent at the top layer.

Fig. 7 illustrates that the highest soil shear strain occurs at the Imogiri borehole, the closest site to the Opak River fault. The most significant shear strain is observed primarily in the middle soil layer, with relatively low stiffness. This phenomenon can be correlated with the Standard Penetration Test (N-SPT) values shown in Figure 4, where the middle layer exhibits lower N-SPT values, indicating reduced soil stiffness. It is well established in geotechnical research that lower soil stiffness leads to more significant displacement, resulting in higher shear strains. In this case, the observed soil shear strain exceeds 0.1%, classifying it as an enormous strain according to Ishihara [1982]. This suggests that the middle layer at the Imogiri site is more susceptible to nonlinear soil behavior, which may influence the site's seismic response and amplification effects during an earthquake.

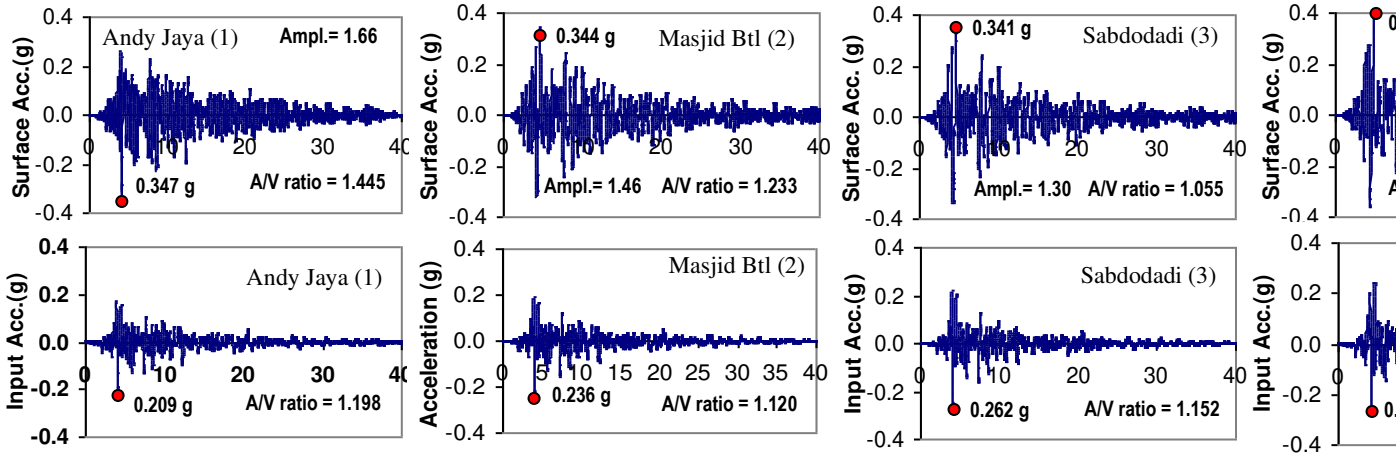

Fig.6. PGA at bedrock and PGA at ground surface

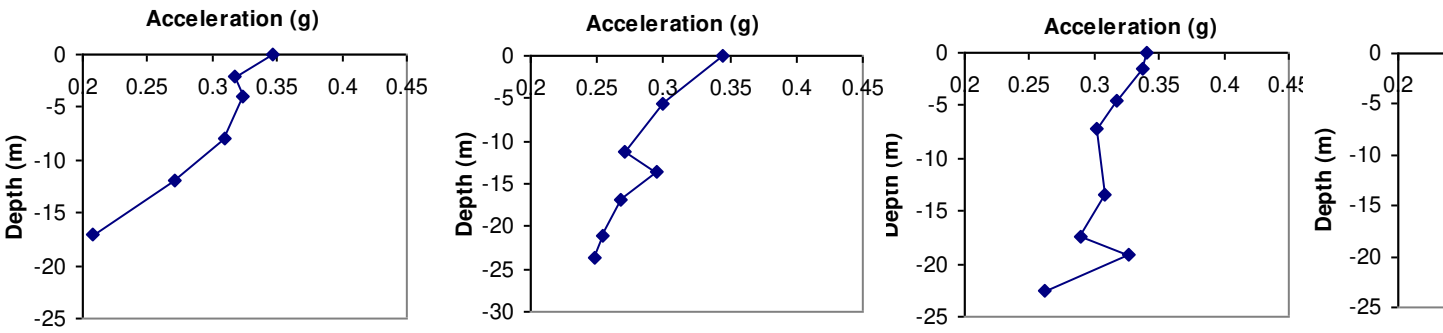

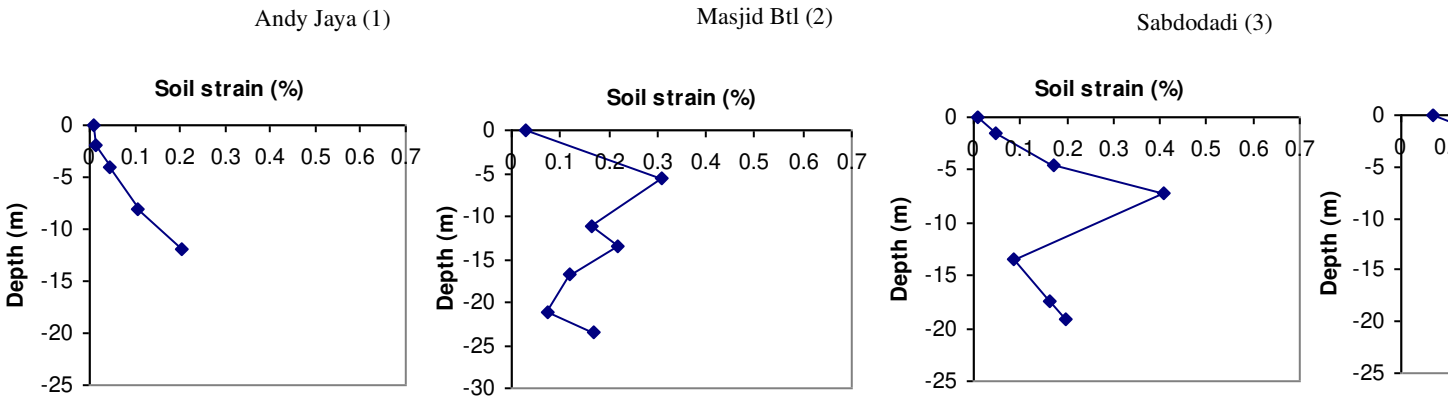

Fig.7. Profile of ground acceleration and strain

6.5. Nonlinear Spectral Amplification

In addition to PGA amplification, Fig. 8 also presents the spectral acceleration amplification for the four boreholes under consideration. One key observation is that, at short vibration periods (T), spectral acceleration amplification tends to remain constant, whereas displacement becomes uniform at more extended periods (T). This result aligns with the findings of Foti et al. [2019] and Bajaj and Anbazhagan [2018]. The maximum spectral accelerations recorded for the Andi Jaya (1), Masjid Btl (2), Sabdodadi (3), and Imogiri (4) boreholes were 1.391 g, 1.176 g, 1.447 g, and 1.486 g, respectively. Among these, the Imogiri (4) borehole exhibited the highest Peak Spectral Acceleration (PSA), as it is the closest to the Opak River fault.

The figure shows that the spectral amplification values were 2,206, 1,650, 1,702, and 1,616 for Andi Jaya, Masjid Btl, Sabdodadi, and Imogiri, respectively. These values were calculated based on the peak-to-peak spectrum ratio. As mentioned earlier, the highest spectral amplification was observed at Andi Jaya, where the soil response remained predominantly elastic. This elasticity resulted in higher computed spectral acceleration amplification compared to PGA amplification.

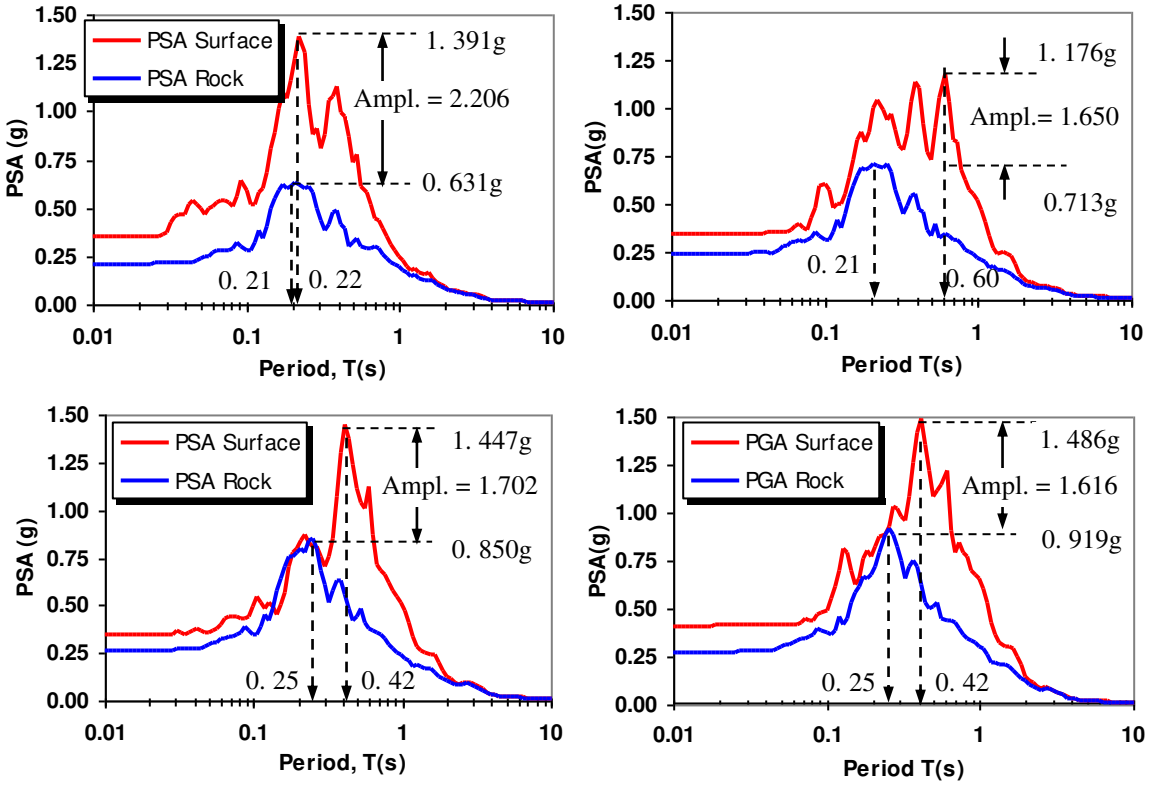

Fig.8. Spectral amplification

The calculated amplification spectrum remains characteristic of the site conditions. Compared to the findings of Kaiser and Massey [2014], the spectral amplification can be classified as moderate to high. According to the data, the borehole locations correspond to areas where the percentage of collapsed buildings and human casualties during the 2006 earthquake was classified as high. This amplification spectrum suggests that the high rate of building collapses and casualties was not solely due to site amplification but was also influenced by other factors. Notably, the quality of building construction materials and the age of the buildings significantly influenced the extent of structural failure and the number of human casualties [Widodo, 2018].

In addition to spectral amplification, Fig. 8 illustrates the vibrating period (T) shift at the ground surface. There is a clear tendency: the softer the soil layer, the more significant the change in the site period (T). As a result, the natural frequency of the earthquake accelerogram at the surface decreases, as indicated by the lower A/V ratio at the ground surface (Fig. 6). Meanwhile, the normalized acceleration response spectrum, or the ratio between the PSA at the ground surface and at bedrock, is presented in Fig. 9. The figure shows that the maximum spectral amplification does not occur at the peak spectrum but instead shifts slightly to the right, around T = 0.50–0.60 s. The spectral amplification observed is greater than the peak-to-peak spectral acceleration ratio.

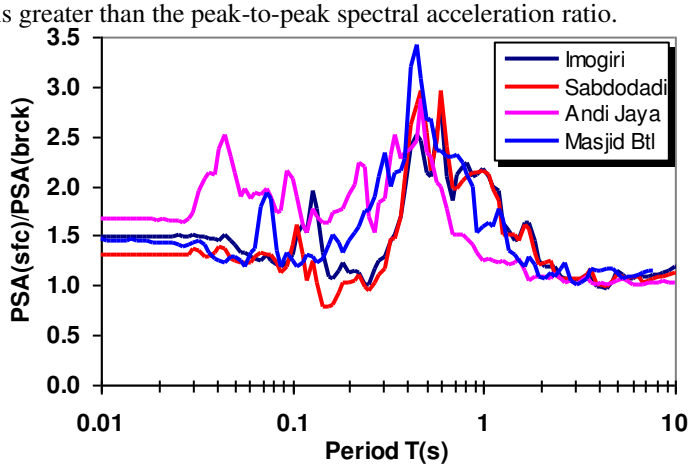

Fig. 9. Normalized acceleration response spectra (spectral ratio surface to bedrock)

6.6. Hysteretic loops of soils

The non-linear behavior of the soil layers is indicated by variations in spring stiffness during the integration process. When shear stress at any given time t is correlated with shear strain, hysteretic loops develop. The hysteretic loops for the top and bottom layers in the four borehole locations are shown in Fig. 10.

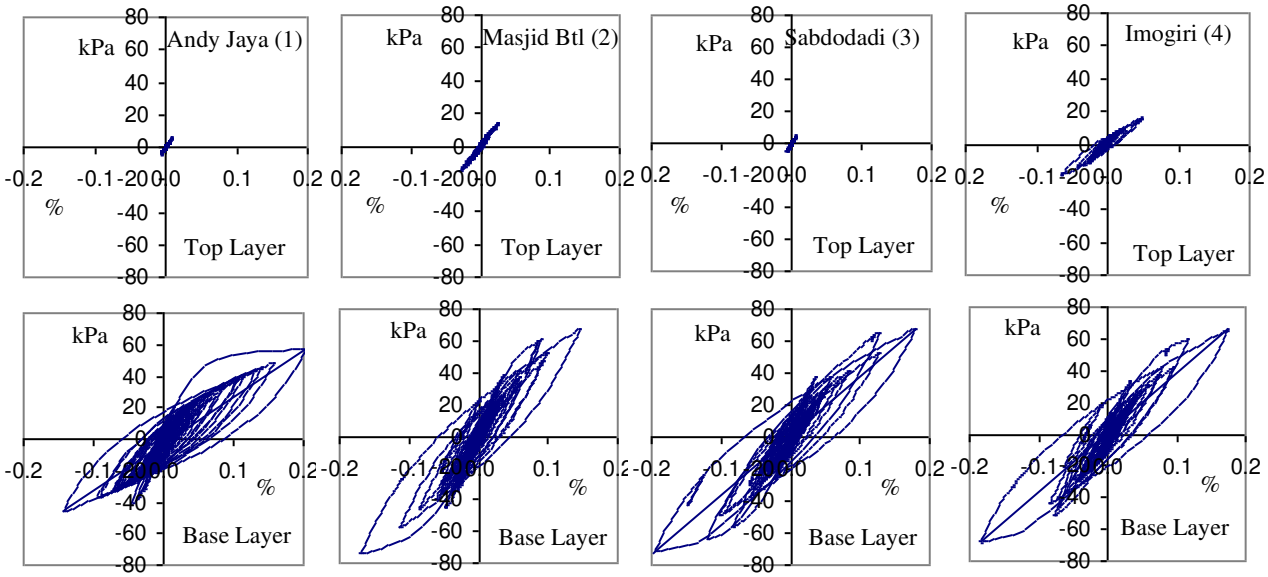

Fig. 10. Hysteretic loops of the top and base layers

As observed in Fig. 10, the top layer experiences only minimal shear stress and shear strain, meaning the soil remains almost elastic. In contrast, the hysteretic loops for the base layers in the four boreholes reveal significant shear strain. The maximum shear strain values in the base layers are 0.204%, 0.169%, 0.197%, and 0.185% for the Andi Jaya, Masjid Btl, Sabdodadi, and Imogiri boreholes, respectively. Since these values exceed 0.1%, they fall into the high shear strain category, as defined by Ishihara [1982].

When shear strain exceeds 0.1%, site response analysis must be conducted using a step-by-step integration method to accurately account for the non-linear soil behavior. This principle has been incorporated into the DEEPSOIL integration scheme. However, certain assumptions are still applied, including (1) shear wave velocity (Vs), (2) shear modulus reduction and damping curves, and (3) actual soil layer thickness, which, in this analysis, can be modeled with layer thicknesses of less than 3 meters per layer. Given these assumptions, further research is needed to achieve greater accuracy and a more comprehensive understanding of soil behavior under seismic loading.

7. Conclusions

Site response analysis across the Opak River fault was conducted using Probabilistic Seismic Hazard Analysis (PSHA), field soil exploration, and vertical propagation of horizontal shear waves. Based on this study, the following conclusions can be drawn:

1) Soil Stratigraphy and Classification
   The soil layers across the four boreholes exhibit consistent stratigraphy, with fine and coarse sand, mainly young Merapi volcanic deposits, dominating the profile. The surface silty loam layer results from rock weathering. Based on N-SPT values, Vs shear wave velocity, and site period (T) criteria, three boreholes (Masjid Btl, Sabdodadi, and Imogiri) are classified as medium soil (SD), while Andi Jaya falls into the hard soil (SC) category. Masjid Btl has the deepest sediment layer before reaching the sandstone and limestone bedrock.
2) Seismic Hazard Analysis
   The Uniform Hazard Spectrum (UHS) was derived at different levels: geometric mean, Maximum Considered Earthquake (MCE), and risk targeted UHS (MCEr). The maximum UHS MCEr at T = 0.2s is: 0.596 g (Andi Jaya), 0.671 g (Masjid Btl), 0.780 g (Sabdodadi), and 0.91 g (Imogiri). The highest UHS MCEr and Peak Ground Acceleration (PGA) were observed at Imogiri, the borehole closest to the Opak River fault.
3) Peak Ground Acceleration (PGA) and Amplification
   Site response analysis using DEEPSOIL software yielded the following PGA values: 0.347 g (Andi Jaya), 0.344 g (Masjid Btl), 0.341 g (Sabdodadi), and 0.411 g (Imogiri). The highest PGA at Imogiri aligns with previous studies, e.g., 0.412g at SMKN 1 Pleret [Widodo 2020] and 0.45g from Modified Mercalli Intensity (MMI) calculations. The peak-to-peak PGA amplification factors were 1.66 (Andi Jaya), 1.46 (Masjid Btl), 1.30 (Sabdodadi), and 1.39 (Imogiri). Similarly, the spectrum amplification factors were 2.26 (Andi Jaya), 1.65 (Masjid Btl), 1.70 (Sabdodadi), and 1.62 (Imogiri). Compared to Kaiser's classification, the amplification levels in this study fall within the low to medium range, except for Andi Jaya, where spectrum amplification is relatively high (2.26). The high building damage rates in these areas were likely due to a combination of moderate soil amplification, high ground acceleration, and poor building construction quality.
4) Soil Response Profile
   PGA values increase toward the surface, indicating that soil layers contribute to peak-to-peak acceleration and amplify the response spectrum. However, shear strain distribution varies, with larger strains occurring in layers with lower stiffness. As a result, (a) the uppermost layers experience lower shear strain, maintaining linear elastic behavior, and (b) the deeper layers exhibit high shear strain, leading to more significant deformation. This finding highlights the non-uniform dynamic response of soil layers, reinforcing the need for site-specific seismic assessments to improve regional structural resilience.

Funding
The authors have not disclosed any funding.

Data availability
Enquiries about data availability should be directed to the authors.

Declarations

Competing interests
The authors have not disclosed any competing interests.

References

Akin, M.K., Kramer, S.L., Topal, T. (2011). Empirical correlations of shear wave velocity (Vs) and Standard Penetration Test (SPT-N) values for various soils in an earthquake-prone area (Erbaa, Turkey). Engineering Geology, Elsevier, Vol. 119, pp. 1-19. doi:10.1016/j.enggo.2011.01.007

Anbazhagan P. 2013. Method for Seismic Microzonation with Geotechnical Aspects. Disaster Advances, Vol. 6, No. 4, pp. 66-85.

Bajaj K, Anbazhagan P, 2018, Ground motion site amplification factor for deep soil deposits sites in Indo-Gangetic Basin, PBD III Vancouver, Earthquake Geotechnical Engineering

Baker J.W. 2008). Introduction to Probabilistic Seismic Hazard Analysis (PSHA), Stanford University, Version 1.3, 72p.

BMKG1 (2019). Katalog Gempa Bumi Siknifikan dan Merusak 1821-2019, Pusat Gempa Bumi dan Tsinami, Badan Meteorologi dan Geofisika, 279 p.

BMKG2 (2010). Katalog Gempa Bumi Siknifikan dan Merusak 1821-2009 (per Wilayah), Pusat Gempa Bumi dan Tsinami, Badan Meteorologi dan Geofisika, 136 p.

Bappenas. (2006). Preliminary Damage and Loss Assessment of the Yogyakarta and Central Java Natural Disaster. The Consultative Group on Indonesia, 123p.

BSN (Badan Standarisasi Nasional). (2018). Tata-cara perencanaan ketahanan gempa untuk struktur bangunan gedung dan non gedung, SNI 1726.

Cornell, C.A. (1978). Engineering Seismic Risk Analysis, Bulletin of the Seismological Society of America. Society of America, 58, No. 5, pp. 1583-1606.

Daryono. (2011). Indeks kerentanan seismik berdasarkan mikrotremor pada setiap satuan bentuk lahan di zona Graben Bantul, Daerah Istimewa Yogyakarta, Gadjah Mada University, 2011 (in Bahasa)

Elnashai, A. S., Kim, S. J., Yun, G. J., & Sidharta, D. (2006). The Yogyakarta Earthquake of May 27, 2006. Mid-America Earthquake Center, University of Illinois at Urbana-Champaign, MAE Report No. 07-2, 57 p.

Fathani T.F, Wilopo W, 2017, Seismic Microzonation Studies Considering Local Site Effects for Yogyakarta City, Indonesia, International Journal of Geomate, Vol.12, Issue 32, pp.152-160, DOI:http://dx.doi.org/10.21660/2017.32.63655

Febriani F, (2014) Subsurface structure of Cimandiri fault zone, West Java Indonesia, Graduate School of Science, Chiba University, 163p,

FEMA P-1050-1, NEHRP Recommended Seismic Provisions for New Buildings and Other Structures (2015), 514 p.

Foti F, Aimar M, Ciancimino A, Passeri F, 2019, Recent development in seismic site response evaluation and micro zonation, , Proceeding of the XVII ECSNGE, Geotechnical Engineering Foundation in the Future, pp.1-26, doi: 10.32075/17ECSMGE-2019-1117

Handayani L, 2019, Active fault zone of the 2006 Yogyakarta earthquake inferred from Tilt derivative analysis of gravity anomalies, Ris. Geo.Tam., Vol.29, No.1, pp.1-11, DOI: 10.14203/risetgeotam2019.v29.1018

Hashash Y.M.A, Musgrove M.I, Harmon J.A, Groholski D.R, Phillips C.A, Park D, 2016, DEEPSOIL 6.1, User Manual

Hashash, Y.M.A., Phillips, C., & Groholski, D.R. (2010). Recent Advances in Nonlinear Site Response Analysis, 5th International Conference on Recent Advances in Geotechnical Engineering and Soil Dynamics.

Huang Y.N, Whittaker A.S, Luco N. (2008). Maximum Spectral Demands in the near Fault Region, Earthquake Spectra, Vol.24, No.1, pp.319-341.

Irsyam, M., Dangkua, D. T., Hendriyawan, Hoedajanto, D., Hutapea, B. M., Kertapati, E. K., Boen, T., & Petersen, M. D. (2008). Proposed seismic hazard map of Sumatra and Java Island and micro-zonation study of Jakarta City, Indonesia. J. Earth Syst. Sci, Vol.117, S2, pp.865-878.

Irsyam M, S Widyantoro S, Natawijaya D.H, Meilano I, Rudyanto A, Hidayati S, Triyoso W, Hanifa N.R, Djarwadi D, Faisal L, Sunarjito. (2017). Peta Sumber dan Bahaya Gempa Indonesia 2017, Pusat Studi Gempa Nasional Pusat Litbang Perimahan dan Pemukiman, 376p.

Ishihara K, 1982, Evaluation of soil properties for use in earthquake response analysis, International Symposium on Numerical Models in Geomechanics, Zurich pp.237-259

Ji K, Ren Y, Wen R, 2017, Site Classification for National Strong Motion Observation Network System (NSMONS) Stations in China Using an Empirical H/V Spectral Ratio Method, Journal of Asian Earth Sciences, Vol. 147, pp. 79-94, http://dx.doi.org/10.1016/j.jseaes.2017.07.032.

Kaiser, A.E., & Massey, C.I. (2014). Site Amplification, polarity, and topographic effects in the Port Hills during the Canterbury earthquake sequence. GNS Science Consultancy Report 121, 31p.

Kempton, J.J., & Stewart, J.P. (2006). Prediction Equation for Significant Duration of Earthquake Ground Motions Considering Site and Near-Source Effects. Earthquake. Spectr. J. 22, No. 4 (2006), pp. 985-1013.

Kijko, A. (2011). Introduction to Probabilistic Seismic Hazard Analysis (Extended version of contribution by A. Kijko, Encyclopedia of Solid Earth Geophysics, Hars Gupta, pp. 1-27).

Kyaw Z.L, S. Pramumijoyo, S. Husein S, T. Fathani T.F, J. Kiyono, and Putra R.R, "Estimation of Subsurface Soil Layers using H / V Spectrum of Densely Measured Microtremor Observations (Case Study : Yogyakarta City , Central Java- Indonesia)," *Int. J. Sustain. Futur. Hum. Secur.*, vol. 2, no. 1, pp. 13–20, 2014. DOI: 10.24910/jsustain/2.1/1320.

Lopez F.A.F, Zamudio J.C.A, Moreno C.O.V, Vasquez V. (2015). Site Response Analysis: A Practical Comparison Among Different Dimensional Approach, Fundamental Application in Geotechnics, pp.1041-1047.doi: 10.3233/978-1-61499-603-3-1041

Loco N (2011). Development of Risk-Targeted Ground Motions for Use in ASCE 7. United States Geological Survey (USGS).

Makrup L.L ,2009, Pengembangan Peta Deagregasi Hazard untuk Indonesia Melalui Pembuatan Software dengan Pemodelan Sumber Gempa 3-Dimensi (3-D), Disertasi Doktor Institut Teknologi Bandung , 235p (in Bahasa)

Madiai C, Facciorusso J, Gargini E, Baglione M, (2016). 1-D versus 2-D site effects from numerical analysis across sections at Berberino di Mugello, Tuscany, Italy. Procedia Engineering, 158, pp. 499-504.

Nguyen, N., Griffin, J., Cipta, A., & Cummins, P. R. (2015). Indonesia's Historical Earthquakes, Modelled Examples for Improving the National Hazard Map, Australian Government, Geoscience Australia, 78 p

Nurwihastuti D.W, Sartohadi J, Mardiatno J.D, Nehren U, and Restu. (2006). Understanding Earthquake Damage Patterns through a Geomorphological Approach: A Case Study of the 2006 Earthquake in Bantul, Yogyakarta, Indonesia. World J. Eng. Technol., vol. 2, no. 3, pp. 61–70, 2014. http://dx.doi.org/10.4236/wjet.2014.23B010.

Partono W, M. Irsyam, S.P.R Wardani. (2017). Development of site class and site coefficient maps of Semarang, Indonesia, using field shear wave velocity data, MATEC Web Conference, 101, 01010, DOI:10.1051/ matecconf/201710105010

Petersen M.D, Dewey J, Hartzell S, Mueller C, Harmsen S, Frankel A. (2004). Probabilistic Seismic Hazard Analysis for Sumatra, Indonesia and across the Southern Malaysian Peninsula, Elsevier.

Pusat Gempa dan Tsunami (PGT), 2019, Katalog Gempa Bumi Siknifikan dan Merusak 1821-2018, Badan Meteorologi dan Geofisika, 278 p.

Seed, H.B., Idriss, I.M. (1969). Influence of Soil Conditions on Ground Motion under Earthquakes, Journal of the Soil Mechanics and Foundation Engineering, ASCE, Vol. 95, pp. 99-138.

Sengara W, Komerdevi Det. (2019). Site-Specific Response Analysis (SSRA) and pairs of ground motion time histories for a site in Jakarta, E3S Web of Conferences, 156,03009, https://doi.org/10.1051/e3sconf/202015603009.

Sunardi, B. (2016). Percepatan tanah sintetis kota Yogyakarta berdasarkan Deagregasi Bahaya Gempa, Jounal Lingkungan dan Bencana Geologi, Vol.6, No.2, pp.211-218, (in Bahasa).

Sutiono, A., Pratistho, B., Prasetyadi, C, Supartoyo. (2018). Opak Fault: A Comparative Review, Earth and Environmental Science, Vol.212, pp.1-8., doi: 10.1088/1755-1315/212/1/012049

Tsuji T, Yamamoto K, Matsuoka T, Yamada Y, Onishi K, Bahar A, Meilano I, Abidin A,Z, 2009, *Earthquake fault of the 26 May 2006 Yogyakarta earthquake observed by SAR interferometry*," Earth, Planets Sp., 61, No. 7, pp. e29-e32.

Widodo, P. (2018). The Estimated PGA Maps of the Mw 6.4, 2006 Yogyakarta, Indonesia Earthquake, Constructed from the Modified Mercalli Intensity (MMI), Bulletin of the New Zealand Society for Earthquake Engineering. Eng., 51, No.2, (2018), pp.92-104.

Widodo, P. (2020). Middle-value ground acceleration map and side effects in the Merapi sedimentary basin under the 2006 Yogyakarta, Indonesia, earthquake. Natural Hazards Journal, 102 (1), 419-443. https://doi.org/10.1007/s11069-020-03932-x.

Widodo P. (2019). Development of synthetic ground motion at a specific site in Yogyakarta town, Indonesia, utilizing the PSHA method. Proceedings of the 4th International Conference on Earthquake Engineering and Disaster Management (4th ICEEDM), Padang, Indonesia, https://doi.org/10.1051/e3conf/202015602011.